Brief Genetics Report

Quantitative Trait Loci for Obesity- and Diabetes-Related Traits and Their Dietary Responses to High-Fat Feeding in LGXSM Recombinant Inbred Mouse Strains

James M. Cheverud,[1] Thomas H. Ehrich,[1] Tomas Hrbek,[1] Jane P. Kenney,[1] L. Susan Pletscher,[1] and Clay F. Semenkovich[2]

Genetic variation in response to high-fat diets is important in understanding the recent secular trends that have led to increases in obesity and type 2 diabetes. The examination of quantitative trait loci (QTLs) for both obesity- and diabetes-related traits and their responses to a high-fat diet can be effectively addressed in mouse model systems, including LGXSM recombinant inbred (RI) mouse strains. A wide range of obesity- and diabetes-related traits were measured in animals from 16 RI strains with 8 animals of each sex fed a high- or low-fat diet from each strain. Marker associations were measured at 506 microsatellite markers spread throughout the mouse genome using a nested ANOVA. Locations with significant effects on the traits themselves and/or trait dietary responses were identified after correction for multiple comparisons by limiting the false detection rate. Nonsyntenic associations of marker genotypes were common at QTL locations so that the significant results were limited to loci still significant in multiple QTL models. We discovered 91 QTLs at 39 locations. Many of these locations (n = 31) also showed genetic effects on dietary response, typically because the loci produced significantly larger effects on the high-fat diet. Fat depot weights, leptin levels, and body weight at necropsy tended to map to the same locations and were responsible for a majority of the dietary response QTLs. Basal glucose levels and the response to glucose challenge mapped together in locations distinct from those affecting obesity. These QTL locations form a panel for further research and fine mapping of loci affecting obesity- and diabetes-related traits and their responses to high-fat feeding. *Diabetes* 53:3328–3336, 2004

From the [1]Department of Anatomy and Neurobiology, Washington University School of Medicine, St. Louis, Missouri; and the [2]Department of Medicine, Washington University School of Medicine, St. Louis, Missouri.

Address correspondence and reprint requests to James M. Cheverud, Department of Anatomy and Neurobiology, Washington University School of Medicine, 660 S. Euclid Ave., St. Louis, MO, 63110. E-mail: cheverud@pcg.wustl.edu.

Received for publication 23 July 2004 and accepted in revised form 25 August 2004.

Additional information for this article can be found in an online appendix at http:// diabetes.diabetesjournals.org.

FDR, false discovery rate; FPR, false-positive rate; QTL, quantitative trait locus.

The prevalence of obesity and its correlates, such as type 2 diabetes, has increased greatly over the last 20 years (1). There has also been a concomitant change in the age of onset for type 2 diabetes, with increasing diagnoses of this disease in children, adolescents, and young adults (2). These secular changes in obesity and diabetes are not due to genetic changes in populations (3), rather they are due to environmental changes in nutrition and activity over time. Even so, there is genetic variation in humans in the response to dietary and activity factors. Some individuals respond strongly to an obesogenic environment by becoming obese, while other individuals remain lean when challenged by the same environment (4). These variations in response to environmental stimuli are, in part, due to genetic variations between people.

Study of differential response to dietary factors in human populations can be challenging because of the difficulty in controlling or accurately recording diet over an extended period of time. Animal studies of the genetic basis for differential response to dietary factors can play an important role in attempts to understand the genetics involved in recent increases in obesity and type 2 diabetes. We have used the cross of inbred mouse strains LG/J and SM/J over the past years to study the genetic architecture underlying complex traits (5), including growth (6,7), obesity (8), and skeletal morphology (5). In continuing studies we have shown that these parental strains vary in obesity- and diabetes-related traits and in responses to dietary fat (9,10). Recently, we documented significant genetic variation in dietary response for fat depot weights, liver weight, leptin levels, fasting glucose levels, and area under the glucose response curve in the LGXSM recombinant inbred (RI) strain set (11). Additionally, genetic variation in dietary response for obesity- and diabetes-related traits was detected in the F_{16} generation of an advanced intercross (AI) line of LG/J and SM/J formed from the same F_2 intercross source population as the RI strains used here (WUSTL:LG,SM-G14), where litters were divided into high- and low-fat diet treatments (12). An AI line is a randomly bred population formed from the F_2

TABLE 1
Composition of high- and low-fat diets

Component	High fat	Low fat
Energy from fat	42%	15%
Casein (g/kg)	195	197
Sugars (g/kg)	341	307
Corn starch (g/kg)	150	313
Cellulose (g/kg)	50	30
Corn oil (g/kg)		58
Hydrogenated coconut oil (g/kg)		7
Anhydrous milk fat (g/kg)	210	
Cholesterol (g/kg)	1.5	
Kilojoules per gram	18.95	16.99

intercross of a pair of inbred strains and maintained at a reasonably large census size ($N > 100$). It is designed to allow fine scale quantitative trait loci (QTLs) mapping using the additional recombinations accumulated over the generations. These earlier results promise success in mapping QTLs in crosses of the LG/J and SM/J inbred mouse lines. Here, we present QTL mapping of obesity- and diabetes-related traits and their responses to increased dietary fat in the LGXSM RI strain set. While a few of these traits have been subject to previous genome-wide QTL scans, many novel traits and dietary responses have not been mapped previously in our cross, including regional fat depots, leptin, cholesterol, free fatty acid, triglycerides, insulin, fasting glucose levels, and response to an intraperitoneal glucose tolerance test. Regions identified here as carrying QTLs will be subject to further research and fine mapping in the WUSTL:LG,SM-G14 AI line.

RESEARCH DESIGN AND METHODS

The LGXSM recombinant inbred line set was produced from the F_2 intercross of LG/J females with SM/J males obtained from Jackson Laboratories. Details of the line formation and history are presented by T.H., L.S.P., R. Alves de Brito, and J.M.C. (unpublished observations). The parental strains were derived from separate selection experiments for high (LG/J) (14) and low (SM/J) (15) adult body weight, respectively. Chai (16) found that differences in body weight were due to many genes ($N \sim 11$) of relatively small additive effect. Therefore, this cross produces a genetic architecture suitable for modeling complex human diseases such as obesity and diabetes, which are also due to many genes of small effect.

The data analyzed here is based on 16 LGXSM RI lines. Strain-, sex-, and diet-specific means and SDs for these traits are reported by Cheverud et al. (11). While sample sizes of specific strain-sex-diet cohorts vary slightly because of differential success in producing experimental animals from our breeding colony, the average cohort sample size was eight animals. Experimental animals remained with their dam, who was fed a standard mouse chow (PicoLab Rodent Chow 20, #5053) until weaning at 3 weeks of age. At this time litters were divided and animals randomly placed into single-sex and dietary treatment groups. Multiple animals were housed in a single cage, with no more than five animals per cage. Animals were fed either the high- or low-fat diet continuously from 3 to 20 weeks. The high-fat diet (Harlan Teklad catalog #TD88137) and the low-fat diet (Research Diets catalog #D12284) compositions are presented in Table 1. All animals were fed ad libitum, and the animal facility was maintained at a constant temperature of 21°C, with 12-h light/dark cycles. All procedures followed the guidelines for the care of laboratory animals at Washington University School of Medicine (Assurance #A-3381-01).

Measurements. Animals were weighed weekly from 1 to 20 weeks of age, after which time they were killed and necropsied. Growth rate was calculated for the adult growth period as the ratio of 20-week weight to 10-week weight. This rate was transformed using the base 10 logarithm before analysis. The adult growth period begins after skeletal growth is complete, and most weight added is in soft tissue, including fat (10).

After 20 weeks of age, animals were subjected to an intraperitoneal glucose tolerance test. Animals were fasted for 4 h, after which a basal blood glucose level was obtained using a Glucometer Dex blood glucose meter (Bayer). Animals were then intraperitoneally injected with 0.01 ml of a 10% glucose solution for every gram of body weight. Additional glucose readings were obtained 15, 30, 60, and 120 min after the initial injection. The graph of the glucose levels over the period of the test are summarized by the area under the curve, which is used as a general measure of an animal's response to a glucose challenge. Lower values indicate a more robust response to glucose. Strain- and sex-specific glucose tolerance curves were presented by Cheverud et al. (11).

At a later time, animals were again fasted for 4 h and anesthetized with sodium pentobarbital, and a terminal blood sample was obtained via cardiac puncture. Blood plasma was separated through centrifugation and analyzed for free fatty acids, cholesterol, triglycerides, leptin, and insulin. Internal organs (liver, spleen, heart, and kidneys) and fat depots (reproductive, renal, mesenteric, and inguinal) were removed and weighed.

Genotypes are available for the RI strains at 506 microsatellite loci spread across the mouse chromosomes with a marker every 2 or 3 cM (T.H., L.S.P., R. Alves de Brito, J.M.C., unpublished observations). Genotypes were scored as corresponding to the LG/J or SM/J parental alleles. Loci showing residual heterozygosity were scored as missing data. A list of the loci scored and their genomic positions is provided in online appendix *A* (available from http://diabetes.diabetesjournals.org). Genotypes for specific strains can be obtained from our laboratory web site (http://thalamus.wustl.edu/cheverudlab/projects.html).

Statistical analysis. The data were first analyzed for QTL effects at each marker scored along the mouse chromosomes using the following nested ANOVA model (17),

$$Y_{ijklm} = \mu + sex_i + diet_j + genotype_k + sex_i \times diet_j + sex_i \times genotype_k + diet_j \times genotype_k + sex_i \times diet_j \times genotype_k + strain_l(sex_i \times diet_j \times genotype_k) + e_{ijklm}$$

where Y_{ijklm} is the phenotype of interest for the m^{th} animal of sex (i), diet (j), and genotype (k) in strain l, and μ is the constant. Strain is nested within the sex-by-diet-by-genotype interaction. The effects of sex, diet, strain, and their interactions were reported by Cheverud et al. (11) and do not vary substantially across the genome scan. The effects of interest here are those due to genotype and its interactions. A significant test for the genotype effect indicates that a QTL affecting the trait of interest resides near the marker. A significant diet-by-genotype interaction indicates that the effect of the QTL varies depending on the diet. Thus, this factor identifies QTLs affecting dietary response. A significant sex-by-genotype interaction identifies a QTL with different effects in males and females. A significant sex-by-diet-by-genotype interaction indicates that a QTL with different effects on male and female dietary responses is present in the region.

Given interactions between genotype and other factors, we also performed genome-wide mapping analyses on each sex and diet cohort separately using the following nested ANOVA model,

$$Y_{ijk} = \mu + genotype_i + strain_j(genotype_i) + e_{ijk}$$

For both ANOVA models, statistical significance was evaluated using the *F* ratio of the mean square for the factor or interaction of interest divided by the mean square of the nested factor, strain (17), typically with 1, 14 d.f. (degrees of freedom).

With 506 ANOVAs involved in the genome scan, some adjustment must be made to account for multiple comparisons. We controlled for multiple comparisons using the false discovery rate (FDR) approach introduced by Storey and Tibshirani (18) and implemented in their QVALUE program. The FDR is the rate that features judged as significant in relation to a threshold are truly null. This is in contrast to the false-positive rate (FPR), which is the rate that truly null features are judged significant. Bonferroni (19) and Monte Carlo (20) simulation–based multiple comparison corrections control FPR. Storey and Tibshirani (18) suggest that the FDR approach is more appropriate in situations where there are a large number of statistical tests to be evaluated and where it is expected that more than one or two of the alternative hypotheses tested are true. Our experience in previous mapping experiments (5) and even evidence from Chai's (16) early breeding experiments is that this cross carries many genes of relatively small effect rather than being dominated by a small number of large-effect genes. We have also previously documented substantial heritability for our traits and their dietary responses in this population (11), so that it is quite likely that there are several instances when the alternative hypothesis of a genetic effect is true. The method is also robust when applied to correlated tests (18). We set the FDR at 5% in our genome-wide scans so that, overall, 5% of the results we deem significant are truly null. An FPR threshold of 5% results in 5% of the truly null results being considered significant. A Bonferroni correction for multiple comparisons applied to this data (19) indicates that probabilities <0.0003 (logarithm of odds [LOD] >3.5) are significant at the 5% level using the FPR criterion.

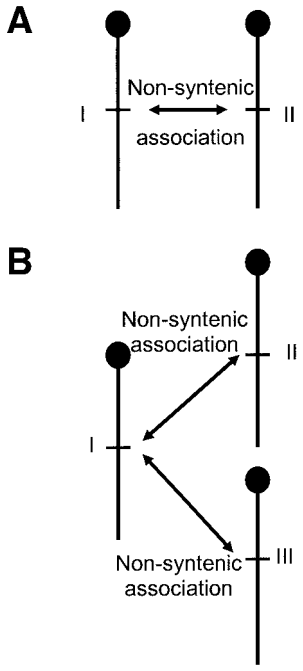

FIG. 1. Illustration of nonsyntenic association between markers on different chromosomes. See text for further details.

One hidden problem in mapping QTLs from small sets of RI strains is the prevalence of nonsyntenic associations between markers (21). These nonsyntenic associations may have either statistical or biological sources. A biological source of nonsyntenic associations is the unintended selection of genomic regions carrying epistatically interacting loci with effects on fertility and/or viability during strain formation. Even in the absence of such selection, nonsyntenic associations will arise as the inevitable statistical result of genome mapping with a relatively small number of strains. With a small number of strains, such as used here, statistical sampling theory predicts that while the average intermarker correlation will be zero, the variance of intermarker correlations will be high, so substantial intermarker correlations will be observed between unlinked markers through genetic drift. With 16 strains the distribution of intermarker correlations among unlinked markers is expected to have a mean of zero and an SD of 0.29, so that each marker is likely to have 23 correlations more than 0.58 or less than −0.58 with other, unlinked markers. Indeed, such nonsyntenic associations are observed in the LGXSM RI strain set (T.H., L.S.P., R. Alves de Brito, J.M.C., unpublished observations). Intermarker correlations are available for inspection at our laboratory website (http://thalamus.wustl.edu/cheverudlab/projects.html). Regardless of whether nonsyntenic associations are due to epistatic selection or statistical sampling, they pose a problem for QTL mapping in RI strains.

The problem caused by nonsyntenic marker association is that a genuine QTL residing at any given genome location will also falsely appear at unlinked sites having nonsyntenic associations with the genuine QTL location. Thus, a genuine QTL will cast its shadow on other, unlinked locations. This problem is illustrated in Fig. 1. In Fig. 1*A* there are two genomic locations, labeled I and II, which are unlinked but happen to be statistically correlated because of sampling error. A genuine QTL at locus I will produce a shadow QTL at locus II because the genotypes at the two loci are correlated. In this situation, we would falsely identify a QTL residing at locus II. If genuine QTLs reside at both locations I and II, then the results obtained at each location will be a combination of the effects at the separate QTLs. If the nonsyntenic association is positive, the effects of the separate QTLs will be added together and appear larger than they really are, inflating the statistical support (LOD score) at both locations. If the nonsyntenic association is negative, the effects of the separate QTLs will cancel each other out, and they will not be detected.

Figure 1*B* illustrates a more complex situation involving three unlinked loci, I, II, and III. There is a nonsyntenic association between loci I and II and between loci I and III, but loci II and III are independent of each other. We can consider a situation in which genuine but very-small-effect QTLs reside at loci II and III with no QTL at locus I. The effects of the genuine QTLs will be combined in the measurements observed at locus I. Thus, locus I will have a larger associated effect and a higher LOD score than either locus II or III. In this case, we are likely to identify a QTL at locus I when it is really just the shadow of the genuine effects at loci II and III. As shown by this example, LOD scores alone cannot be used to resolve problems caused by nonsyntenic associations. Here the location with the highest LOD score (I) would be a shadow of genuine QTL at other locations (II and III). One can imagine many even more complex patterns of nonsyntenic association, especially in situations where there are several genuine QTLs.

One can determine which QTLs may be genuine and which may be their shadows by fitting a multiple QTL model that simultaneously measures the independent effect of each location while controlling for the effects of its associates. A location that remains significant even when controlling for unlinked correlated markers is likely to be a genuine QTL. The remaining locations that are no longer significant in a multiple QTL model are considered to be shadow QTLs. As a caveat, it may be that genuine QTLs really do reside at our shadow sites but that their intercorrelations are too high to separate their independent effects with the small samples available. Further experiments are necessary to securely eliminate perceived shadow sites as locations with genuine effects on the phenotypes of interest.

We addressed the problem of nonsyntenic associations in the LGXSM RI strain set by examining the observed marker intercorrelations between QTL localities. We then applied multiple QTL models to sets of highly intercorrelated localities ($r > 0.50$) and retained the individual QTLs that still had significant effects in the presence of correlated markers. These select markers were then combined into one multiple QTL model, and QTL locations were retained if they remained significant at the 5% level. The number of independent QTLs that can be supported with our data in any single multiple QTL model is limited to five or six locations by the number of strains and the levels of intermarker correlations. Thus, if locations identified here as genuine QTL fail to replicate in later experiments, their shadow sites should be examined more closely. Also, it is important to note that some sites with very strong support in a single QTL model may not be included in the final genuine QTL set because of their relatively high intercorrelations with other significant localities.

RESULTS

Our genome-wide scan has identified a large number of significant QTLs scattered across the genome. These QTLs and their confidence regions are displayed graphically in online appendix *A*. Specific QTL locations, confidence support regions, associated LOD scores, and least squares means for the LG/J and SM/J genotypes for each diet and sex group are presented in online appendix *B* and summarized in Table 2. All loci listed have probabilities below the 5% *q*-value threshold. There are a total of 53 separate map locations with from 1 to 13 traits per location for a total of 284 trait-specific QTLs.

However, there are many significant nonsyntenic associations between these QTLs. After application of multiple QTL models, 91 QTLs remain at 39 separate map positions affecting 1 to 10 traits per location. QTL locations considered genuine are listed separately from those considered as shadows in Table 2 and appendix *B*. Genuine QTLs that are supported at the genome-wide Bonferroni level (LOD >3.5) are considered strongly significant and are underlined in Table 2. The remaining genuine QTL should be considered as suggestive. Associated genuine QTLs with correlations more than 0.5 or below −0.5 are also listed for each of the shadow QTL sites in online appendix *B*. Approximately two-thirds of the original QTLs may represent shadow sites, an average of two shadows for each genuine QTL.

For most traits, the LG/J allele leads to a higher value (58% of the time), but the SM/J allele leads to a higher value at ~42% of the QTLs. For a few traits, including free fatty acid level, triglyceride level, fasting glucose level, and area under the glucose response curve, the SM/J allele leads to higher levels in more than half of the QTLs.

A few sex-specific QTLs were identified (eight trait QTLs). The male-specific QTL involving fasting glucose

TABLE 2
Chromosomal locations of QTLs mapped in the LGXSM RI strain set on a high- and low-fat diet

Chromosome 1	
296–478	Renal; **shadow:** tail, {spleen}*, *trig*†
74–415	Insulin; **shadow:** totfat, renal, mesen, ing, leptin, necwt, chol, tail
48–103	Totfat, repro, renal, mesen, ing, leptin, necwt, chol, tail; **shadow:** *adult*‡, {*kidney*}
196–507	Chol, heart; **shadow:** totfat, repro, *renal*, mesen, necwt, *trig*
113–155	Insulin; **shadow:** {AUC20}♂, kidney, heart, spleen
Chromosome 2	
1–119	{Kidney}, adult, **shadow:** {AUC20}
370–409	**Shadow:** AUC20, mesen, {*kidney*}, {trig}♀
412–265	**Shadow:** totfat, repro, renal, mesen, ing, leptin, necwt, *adult*, chol
Chromosome 3	
60–167	*Mesen*, necwt, chol; **shadow:** *totfat*, *renal*
182–106	{Trig}; **shadow:** adult, *heart*, {kidney}, {tail}
106–111	Spleen; **shadow:** *totfat*, *repro*, {chol}
Chromosome 4	
235–89	*Repro*; **shadow:** *totfat*, *renal*, {G020}, {AUC20}
133–135	**Shadow:** {G020}♂, {liver}
332–203	**Shadow:** *renal*, *mesen*, {tail}
148–150	**Shadow:** spleen, {FFA}
Chromosome 5	
47–352	{*Kidney*}; **shadow:** totfat, *renal*, mesen, leptin, chol, {spleen}
267–188	{*Trig*}; **shadow:** {spleen},
168–169	{FFA}
Chromosome 6	
236–186	{G020}, {AUC20}; **shadow:** spleen, {tail}
209–14	FFA, tail; **shadow:** {adult}, trig
198–201	**Shadow:** {mesen}, {leptin}, kidney, spleen, tail
Chromosome 7	
21–346	Heart; **shadow:** {chol}, {trig}, {*FFA*}♀, spleen
S1–281	**Shadow:** kidney
238-S4	*Mesen*, adult, tail; **shadow:** *totfat*, *repro*, *renal*, *ing*, *leptin*, necwt
Chromosome8	
58–80	{Spleen}; **shadow:** {trig}, {kidney}
312–56	{*Totfat*}, {*repro*}, {*renal*}, {mesen}, {*ing*}, {*leptin*}, {*necwt*}; **shadow:** {*adult*}♀, trig, {tail}
Chromosome 9	
218–289	{FFA}; **shadow:** {*trig*}, {chol}
266–267	**Shadow:** {adult}, tail
201–19	**Shadow:** {*totfat*}, {*repro*}, {*renal*}, {*mesen*}, {*ing*}, {*leptin*}, {*necwt*}, {*heart*}
Chromosome 10	
213–65	**Shadow:** {trig}, {FFA}♀, tail♂
295–305	Totfat, repro, renal, mesen, ing, necwt, *liver*, heart; **shadow:** kidney, spleen, tail
Chromosome 11	
71–173	{*Trig*}; **shadow:** G020♂, AUC20, {FFA}, spleen
349–41	Totfat; **shadow:** *repro*, mesen, ing, necwt, tail
285–48	{*Liver*}, kidney; **shadow:** {G020}♂, {AUC20}
Chromosome 12	
145–153	{Adult}, {chol}; **shadow:** {totfat}, {mesen}, {ing}, {necwt}
2–6	Spleen, *heart*; **shadow:** totfat, repro, renal, kidney, tail
231-S2	Adult; **shadow:** *totfat*, *renal*, *mesen*, ing, necwt, chol, *liver*
Chromosome 13	
1–134	*Liver*
207–64	Chol, trig; **shadow:** totfat, renal, mesen, ing, leptin, necwt♀, spleen, tail
7–144	Kidney
147–35	**Shadow:** *totfat*, repro, *renal*, mesen, necwt, chol, *heart*
Chromosome 14	
S1–266	{FFA}, kidney; **shadow:** spleen
Chromosome 15	
13-S2	{*Heart*}; **shadow:** tail
203–66	**Shadow:** {*totfat*}, {*repro*}, {*renal*}, {mesen}, {adult}♀, trig
2–42	{Chol}, {spleen}; **shadow:** G020, AUC20
Chromosome 16	
28–152	{Necwt}♀; **shadow:** {totfat}, {renal}♀, {mesen}, {ing}, {leptin}, {liver}, {spleen}, {kidney}, {tail}, {AUC20}
Chromosome 17	
19–115	Kidney, adult, chol; **shadow:** *totfat*, *repro*, *renal*, *mesen*, *ing*, leptin, *necwt*, insulin, {AUC20}, *liver*

Continued on following page

TABLE 2
Continued.

Chromosome 18	
64–94	**Shadow:** {trig}, *liver*
17–213	Totfat, *ing*, leptin; **shadow:** *repro*, mesen, necwt, chol♀, tail
Chromosome 19	
43–16	G020♂, AUC20, liver; **shadow:** kidney, spleen
111–137	**Shadow:** *repro*, tail
Chromosome X	
55–10	{G020}, {AUC20}; **shadow:** trig, kidney
121–186	{*Totfat*}♀, {*repro*}♀, {*renal*}♀, {*mesen*}♀, {leptin}♀, {necwt}, {chol}♀, {insulin}, {*liver*}, {spleen}; **shadow:** {ing}, {adult}♀

Chromosomal locations are identified by markers spanning support intervals. Marker names are *DXMitY*, where X is the chromosome number and Y is the marker number given in the table. QTLs are listed first followed by potential shadow QTLs (**shadow**). Trait designations are given in the note indicated with an asterisk. Underlined traits are rated as genome-wide significant QTLs, while traits not underlined should be considered as suggestive QTLs. *No parentheses for QTLs where the LG/J allele leads to higher trait values and {} enclose QTLs where the SM/J allele leads to higher values. ‡Adult = growth from 10–20 weeks. †Italic font indicates that the QTL is diet dependent, only being apparent on a high-fat diet. ♂, male-specific QTL; ♀, female-specific QTL. AUC20, area under glucose tolerance curve at 20 weeks; chol, cholesterol level; FFA, free fatty acid level; G020, fasting glucose level at 20 weeks; heart, heart weight; ing, inguinal fat depot weight; insulin, fasting insulin level at 20 weeks; kidney, kidney weight; leptin, fasting leptin level at 20 weeks; liver, liver weight; mesen, mesenteric fat depot weight; necwt, body weight at necropsy; renal, renal fat depot weight; repro, reproductive fat depot weight; spleen, spleen weight; tail, tail length; totfat, sum of the four fat depots; trig, triglyceride levels.

level is on chromosome 19. There is a female-specific QTL for necropsy weight on chromosome 16, and a female-specific QTL for fat depot weights, leptin, and cholesterol levels on distal chromosome X.

Over the whole set of QTL trait combinations, ~34% were only observed on the high-fat diet. The other 66% of the QTLs did not respond to the high-fat diet by increasing the difference between the LG/J and SM/J allelic effects. The typical pattern for the dietary response QTLs is that there was no significant effect of the alleles on a low-fat diet but that a QTL could be detected when the animals were fed a high-fat diet. Only one QTL, kidney weight on proximal chromosome 5, was significant solely on a low-fat diet. At this locus the original difference in kidney size (LG/J > SM/J) is eliminated by the stronger response of the SM/J genotype to the high-fat diet.

The percentage of increase in the number of QTLs on a high-fat diet relative to diet-unresponsive QTLs varies considerably, depending on the trait considered. The traits with the most dietary response loci were the fat depot weights, reproductive fat depot (4:1, four dietary response loci to one unresponsive locus), renal fat depot (3:2), mesenteric fat depot (4:2), inguinal fat depot (3:1), and total fat weight (4:2). The liver also had several diet responsive loci (3:2), while the other organs, including heart, spleen, and kidneys, together only rarely showed a dietary response (4:15). Some dietary response was also noted for leptin levels (1:3), necropsy weight (2:4), and triglyceride and free fatty acid levels (2:8). The remaining traits did not have QTLs with significantly different effects on the high- and low-fat diets.

There were, on average, two to three traits mapping to each QTL location. Whether this joint mapping actually represents pleiotropy or the close linkage of different genes affecting the traits cannot be determined directly from this data but requires finer mapping with a larger number of available recombinations. However, there are distinct patterns in the joint mapping of traits. A set of traits often found mapping together include the four fat depots (reproductive, renal, mesenteric, and inguinal) and leptin levels. These general obesity loci are located in mid-chromosome 1, distal chromosome 8, distal chromosome 10, and the distal X chromosome. Of these four QTLs, only that on chromosome 1 failed to show an interaction with diet. Other locations with effects on individual fat depots include the renal fat depot on proximal chromosome 1, the mesenteric fat depot on proximal chromosome 3 and distal chromosome 7, the reproductive fat depot on proximal chromosome 4, and the inguinal fat depot on distal chromosome 18. A QTL for total fat depot weight maps to the middle of chromosome 11, although this site is classified as a shadow site for several of the individual depots. Necropsy weight, liver weight, and cholesterol level also map at some of the obesity QTLs. Fasting glucose levels and area under the glucose response curve map together at three QTLs on proximal chromosome 6, proximal chromosome 19, and on the X chromosome and are not found mapping jointly with the fat depots.

DISCUSSION

The large number of QTLs found here relative to other studies is due to a variety of circumstances. First, these strains were known to differ in many genes of relatively small effect from earlier genetic studies (6,7,16). Second, a large number of related traits were measured, including four separate fat depots, organ weights, and serum levels for obesity- and diabetes-related factors. Third, these RI lines carry higher levels of recombination than those found in an F_2 intercross population, allowing slightly finer mapping and better distinction of multiple QTLs along a chromosome. Furthermore, significance thresholds were set using the false detection rate threshold (18), which is more liberal than the usual Bonferroni-style correction. This threshold is appropriate in situations where previous data, such as earlier QTL studies on this cross (6–8) and the heritability of these traits across the RI strains (11), indicate that a null hypothesis of no effect at any location is not tenable. A more stringent, Bonferroni-style correction would consider LOD scores over ~3.5 as significant. This more stringent level would eliminate 60% of the

TABLE 3
Selected positional candidate genes within the support intervals of obesity and glucose level QTLs

Chromosome	Trait	Marker(s)	No. of Genes*	ID	Name
1	Obesity	*D1Mit187* {*D1Mit10*, *D1Mit139*, 8.4 cM}	134	*Avpr1b*	Vasopressin V1B receptor
				Insig2	Insulin-induced gene 2
				Hdlbp	HDL binding protein
				Capn10	Calpain 10
				Pfkfb2	6-Phosphofructo-2-kinase/fructose-2,6-biphosphatase 2
				Daf1	Complement decay-accelerating factor, GPI-anchored precursor
				Dbi	Acyl-CoA-binding protein (ACBP)
				Tnfrsf11a	Tumor necrosis factor receptor superfamily member 11A precursor
8	Obesity	*D8Mit89* {*D8Mit316*, *D8Mit13*, 11 cM}	69	*Trhr2*	Thyrotropin-releasing hormone receptor 2
				Mc1r	Melanocortin-1 receptor
10	Obesity	*D10Mit266* {*D10Mit178*, *D10Mit103*,11 cM}	54	*Frs2*	Fibroblast growth-factor receptor substrate 2
				Avpr1a	Vasopressin V1A receptor
				Tph2	Tryptophan 5-hydroxylase 2
X	Obesity	*DXMit186* {*DXMit121*, *DXMit186*, 2 cM}	34	*Grpr*	Gastrin-releasing peptide receptor
				Ace2	ACE precursor 2
				Tlr8	Toll-like receptor 8 precursor
				Tlr7	Toll-like receptor 7 precursor
6	Glucose	*D6Mit96* {*D6Mit175*, *D6Mit186*, 2 cM}	38	*Fabp1*	Fatty acid–binding protein, liver
19	Glucose	*D19Mit28* {*D19Mit43*, *D19Mit16*, 16 cM}	37	*Stx3*	Syntaxin 3
X	Glucose	*DXMit173* {*DXMit144*, *DXMit121*, 47 cM}	238	*Gpr50*	Melatonin-related receptor
				Avpr2	Arginine vasopressin receptor 2
				G6pdx	Glucose-6-phosphate 1-dehydrogenase X
				Pgr15l	Neuropeptide Y receptor
				Gilz	Glucocorticoid-induced leucine zipper protein
				Irs4	Insulin receptor substrate-4
				Capn6	Calpain 6
				Mbtps2	Mammalian sterol-regulatory element–binding protein (SREBP) site 2 protease

Support interval marker boundaries and length are given inside brackets { }. *Number of known genes within the support interval.

trait-QTL combinations and ~25% of the 52 QTL locations mapped here and can be easily applied to the results in online appendix *B*. Clearly, those QTLs and effects associated with higher LOD scores are more certain and the most likely to be followed up first.

The large number of shadow QTLs found in this analysis points out the critical importance of considering the effects of nonsyntenic association on the interpretation of genome-wide QTL mapping in RI strains. To our knowledge, this has not been directly addressed in earlier QTL mapping studies. Using a liberal definition of shadow sites, we detected two shadows for each genuine QTL mapped. Distinguishing between actual and shadow QTLs can prove difficult, especially when there is a high intercorrelation between the genomic locations involved. Here, we used the relative probabilities of the locations in multiple QTL models to distinguish likely genuine from shadow sites. Random multicolinearity due to high multiple correlations between QTL sites limits the number of QTLs that can be detected in this population of RI strains to approximately five or six QTLs. Some of the sites identified here as shadow sites are likely to contain genuine QTL, and if a site identified as a genuine QTL in this study fails to replicate, its associated shadow site(s) provide logical candidate positions.

Pleiotropic patterns can only be roughly judged from this data because mapping is not precise, making it difficult to distinguish between traits mapping to the same region of the genome because of pleiotropy or because of close linkage between separate genes affecting separate traits. However, we found the four fat depots and leptin levels map together much more often than expected by chance. It is likely that this colocation is due to the pleiotropic effects of individual genes in each of these regions. This set of traits also showed very high genetic correlations in quantitative comparisons of the RI strains (11). Necropsy weight and cholesterol levels are also often affected by locations affecting the fat depots and leptin levels.

There were four genuine obesity QTLs affecting multiple fat depots, residing on chromosomes 1, 8, 10, and X, with the last three being dietary response loci only showing an effect on the high-fat diet. The chromosome 1 obesity QTL also affects serum cholesterol levels. There are many positional candidate genes in this QTL region ($n = 134$); however, several stand out as being potentially involved in obesity and related traits. These select positional candidate genes are listed in Table 3. Genes closest to the chromosome one QTL peak include tumor necrosis factor receptor superfamily member 11A precursor (*Tnfrsf11a*), Acyl-CoA binding protein (*Dbi*), and insulin-induced gene 2 (*Insig2*). The chromosome 8 obesity QTL only affected the fat depots, leptin level, and body weight. It maps to a relatively narrow region containing 69 genes, two of

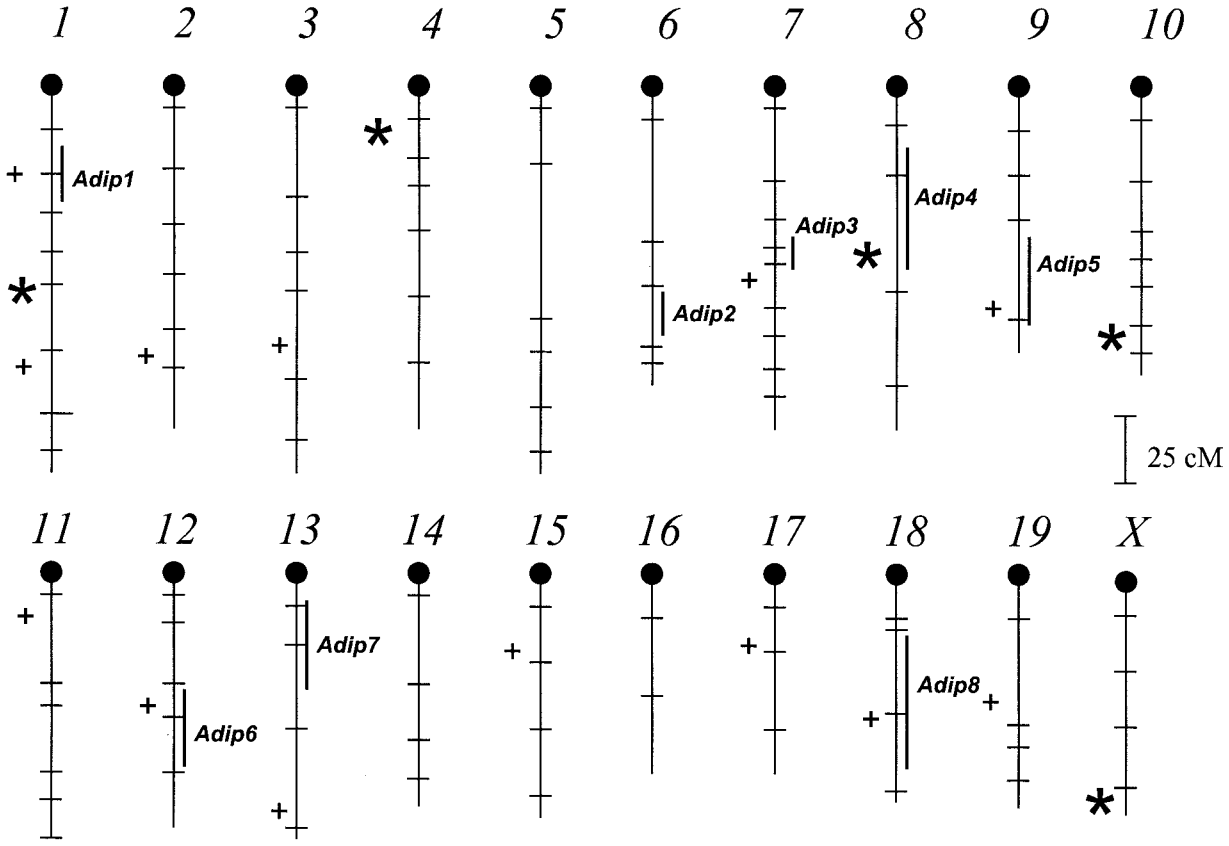

FIG. 2. Correspondence between obesity loci mapped in the LG/J by SM/J F2 intercross (8) and in the present study. QTLs identified in the F_2 intercross are identified by name (*Adip1–8*). Obesity QTLs judged as genuine in this study are indicated by an asterisk (*), while shadow sites are indicated by a plus sign (+).

which, thyrotropin-releasing hormone receptor 2 (*Trhr2*) and melanocortin-1 receptor (*Mc1r*), have known interactions with obesity-related pathways. The chromosome 10 obesity QTL also affects heart and liver weights and maps to a region containing 54 genes. Especially interesting positional candidates include fibroblast growth-factor receptor substrate 2 (*Frs2*), a vasopressin receptor (*Avpr1a*), and tryptophan 5-hydroxylase 2 (*Tph2*). The X chromosome obesity QTL had effects restricted to females and pleiotropic effects on serum cholesterol levels and liver, heart, and spleen weights. It maps to a narrow region at the distal end of the X chromosome containing 34 genes including a gastrin-releasing peptide receptor (*Grpr*), an ACE precursor (*Ace*II), and two toll-like receptor precursors (*Tlr7* and *Tlr8*).

The two measures of serum glucose, fasting glucose level and area under the glucose response curve, also usually map together. Interestingly, these locations do not coincide with the obesity QTLs, supporting the relative independence of glucose level and obesity indicated by the low genetic correlations observed between glucose levels and obesity phenotypes in the RI strains (11). In this strain set, obesity- and diabetes-related traits are most often affected by different genes. The chromosome 6 glucose QTL maps to a narrow region containing 38 genes including the fatty acid–binding protein for the liver (*Fabp1*). The chromosome 19 glucose QTL also affects liver weight. It maps to a narrow region at the proximal end of the chromosome containing 37 genes, including a syntaxin gene (*Stx3*). The X chromosome glucose QTL maps to a large portion of the chromosome containing 238 known genes. Interesting candidate genes mapping nearest the QTL peak include glucocorticoid-induced leucine zipper protein (*Gilz*), insulin receptor substrate 4 (*Irs4*), and calpain 6 (*Capn6*).

We also located a large number of dietary response QTLs, and ~34% of our QTLs had no effect on the low-fat diet but had strong significant effects among animals fed a high-fat diet. These genes can be considered to be differentially responsive to the amount of dietary fat and would be especially important for modeling the increase in obesity with changing dietary habits in modern human populations. While animals of all genotypes respond to the high-fat diet at these dietary response loci, those carrying one genotype respond more strongly than those carrying the other. Approximately 50% of the dietary response QTLs had larger responses for the LG/J allele, with the remaining dietary response QTLs having a larger response for the SM/J allele. The remaining 66% of the QTLs did not show a differential dietary response for the LG/J and SM/J alleles. Usually this occurred because both genotypes responded in the same fashion and to the same extent to a high-fat diet. Only rarely were QTLs detected on a low-fat diet that did not have any effect on the high-fat diet (1% of trait QTLs). The traits that showed relatively more dietary response QTLs also tended to have higher dietary response heritabilities (11) ($r = 0.47$).

Dietary response QTLs showed a pattern of pleiotropy

similar to that for the trait QTLs themselves. The four fat depots, leptin, and necropsy weight tended to respond to the high-fat diet as a group, probably due to the pleiotropic effects of dietary response QTLs.

Most of the traits studied here have never been mapped in the LG/J by SM/J cross. Of special interest is the earlier study mapping QTLs for the reproductive fat depot weight at 10 weeks in the F_2 intercross population (8). This fat depot was also mapped here but at 20 weeks rather than 10 weeks. Also, none of the animals in the present study were bred, while most F_2 females had been bred and produced litters before necropsy. An additional difference is that the F_2 animals were reared on a single diet, most closely resembling the low-fat diet used here. While the reproductive fat depot weights reported here are not fully comparable with those measured in the F_2 intercross population, it is worth considering the present results in relation to these earlier ones. Locations of the eight adiposity loci reported by Cheverud et al. (8) and the genuine and shadow sites reported here are illustrated in Fig. 2. *Adip4* on chromosome 8 mapped in the F_2 generation has a corresponding genuine QTL in the RI strains. Most of the previously mapped adiposity QTLs are at sites identified here as potential shadow sites, including Adip1, *Adip3*, *Adip5*, *Adip6*, and *Adip8*. The replication of earlier F_2 results as mirror sites with the RI strains argues for these sites actually carrying QTLs affecting obesity. The failure of sites identified in the F_2 to be identified as genuine in this study is due to multicolinearity due to nonsyntenic associations. While *Adip2* does not replicate in this study, its location is strongly supported by mapping in the F_{10} generation of the LG/J by SM/J randomly mated advanced intercross lines (unpublished data). Additionally, while *Adip7* failed to replicate in this present study, analyses of dietary response in the F_{16} generation of the advanced intercross line support this QTL's effect on obesity- and diabetes-related traits (unpublished data). The genuine fat depot QTLs identified here correspond to locations found to affect 10-week body weight but not reproductive fat depot weight in the F_2 intercross, including the QTLs on chromosomes 1, 4, and 10 (7,8). Chromosome X was not included in our earlier mapping studies due to relative lack of polymorphic markers.

Anunciado et al. (22–24) have mapped a series of traits, including some mapped here, in RI lines and an F_2 intercross between SM/J and A/J mouse strains. Since this cross shares a parent with the cross reported here, it is possible that some of the same QTLs may be discovered in both studies. Mapping in the SMXA RI strains suggested a QTL for body weight at the middle region of chromosome 1 and a QTL for insulin levels on chromosome 17 that can be roughly paired with QTLs reported here (22), although it appears in this study that the chromosome 17 site is a shadow site for the distal X chromosome QTL. Body weight QTLs that correspond to related traits mapped here on chromosomes 2, 6, 7, 8, 18, and 19 were also mapped in the SM/J $\times$ A/J F_2 intercross, with only the QTL on chromosome 15 not replicating across studies (23). Common QTLs were mapped for triglyceride levels on chromosome 8 and for cholesterol levels on chromosomes 1, 3, and 17 in the same F_2 population (24). While these related crosses replicate each other to some extent, there are still many independent QTLs mapped in these studies. The variance for many traits among the SMXA RI strains appears lower than for the LGXSM RI strains, making QTL detection less powerful in the SMXA RI strains.

The results presented here suggest that fine mapping QTLs for obesity- and diabetes-related traits will be quite successful in the LG/J $\times$ SM/J intercross. We reared a F_{16} advanced intercross line (WUSTL:LG,SM-G14) on both a low-fat and a high-fat diet. This population can be used to follow up the results reported here. Ehrich et al. (25) have fine mapped the proximal portion of chromosome 13 for dietary response QTLs and located a region with differential effects on liver weight, reproductive fat depot weight, and insulin levels, depending on diet. At this locus, SM/J homozygotes respond more strongly to the high-fat diet than LG/J homozygotes. Further loci can be fine mapped using the QTL map presented here as a guide. More precise QTL positions will also allow the positional candidate genes reported here to be validated or removed from further consideration.

ACKNOWLEDGMENTS

This work was supported by National Institutes of Health Grants DK55736, DK52514, HL58427, and RR15116 and Washington University's Clinical Nutrition Research Unit (DK56341) and its Diabetes Research Training Center (2 P60 DK20579).

REFERENCES

1. Mokdad AH, Ford ES, Bowman BA, Dietz WH, Vinicor F, Bales VS, Marks JS: Prevalence of obesity, diabetes, and obesity-related health risk factors, 2001. *JAMA* 289:76–79, 2003
2. Must A, Spadano J, Coakley EH, Field AE, Colditz G, Dietz WH: The disease burden associated with overweight and obesity. *JAMA* 282:1523–1529, 1999
3. Yanovski JA, Yanovski SZ: Recent advances in basic obesity research. *JAMA* 282:1504–1506, 1999
4. Seidell JC: Dietary fat and obesity: an epidemiologic perspective. *Am J Clin Nutr* 67:546S–550S, 1998
5. Cheverud JM: Genetic architecture of quantitative variation. In *Evolutionary Genetics: Concepts and Case Studies*. Fox CW, Wolf JB, Eds. Oxford, U.K., Oxford University Press, 2005
6. Cheverud JM, Routman EJ, Duarte FM, van Swinderen B, Cothran K, Perel C: Quantitative trait loci for murine growth. *Genetics* 142:1305–1319, 1996
7. Vaughn TT, Pletscher LS, Peripato A, King-Ellison K, Adams E, Erikson C, Cheverud JM: Mapping quantitative trait loci for murine growth: a closer look at genetic architecture. *Genet Res* 74:313–322, 1999
8. Cheverud JM, Vaughn TT, Pletscher LS, Peripato A, Adams E, Erickson C, King-Ellison K: Genetic architecture of adiposity in the cross of large (LG/J) and small (SM/J) inbred mice. *Mamm Genome* 12:3–12, 2001
9. Cheverud JM, Pletscher LS, Vaughn TT, Marshall B: Differential response to dietary fat in large (LG/J) and small (SM/J) inbred mouse strains. *Physiol Genomics* 1:33–39, 1999
10. Ehrich TH, Kenney JP, Vaughn TT, Pletscher LS, Cheverud JM: Diet, obesity, and hyperglycemia in LG/J and SM/J Mice. *Obes Res* 11:1400–1410, 2003
11. Cheverud JM, Ehrich TH, Kenney JP, Pletscher LS, Semenkovich CF: Genetic evidence for discordance between obesity and diabetes-related traits in the LGXSM recombinant inbred mouse strains. *Diabetes* 53:2700–2708, 2004
12. Ehrich TH, Kenney JP, Pletscher LS, Cheverud JM: Genetic variation and co-inheritance of dietary response in a LG×SM murine model of obesity. *Genet Res.* In press
14. Goodale H: A study of the inheritance of body weight in the albino mouse by selection. *J Hered* 29:101–112, 1938
15. MacArthur J: Genetics of body size and related characters. I. Selection of small and large races of the laboratory mouse. *Am Nat* 78:142–157, 1944
16. Chai CK: Analysis of quantitative inheritance of body size in mice. II. Gene action and segregation. *Genetics* 41:167–178, 1956

17. Sokal RS, Rohlf FJ: *Biometry*. New York, W.H. Freeman and Company, 1995
18. Storey JD, Tibshirani R: Statistical significance for genomewide studies. *Proc Natl Acad Sci U S A* 100:9440–9445, 2003
19. Cheverud JM: A simple correction for multiple comparisons in interval mapping genome scans. *Heredity* 87:52–58, 2001
20. Churchill G, Doerge R: Empirical threshold values for quantitative trait mapping. *Genetics* 138:963–971, 1994
21. Williams RW, Gu J, Qi S, Lu L: The genetic structure of recombinant inbred mice: high resolution consensus maps for complex trait analysis. *Genome Biol* 2:0046.1–0046.18, 2001
22. Anunciado RVP, Ohno T, Mori M, Ishikawa A, Tanaka S, Horio F, Nishimura M, Namikawa T: Distribution of body weight, blood insulin and lipid levels in the SMXA recombinant inbred strains and the QTL analysis. *Exp Anim* 49:217–224, 2000
23. Anunciado RVP, Nishimura M, Mori M, Ishikawa A, Tanaka S, Horio F, Ohno T, Namikawa T: Qunatitative trait loci for body weight in the intercross between SM/J and A/J mice. *Exp Anim* 50:319–324, 2001
24. Anunciado RVP, Nishimura M, Mori M, Ishikawa A, Tanaka S, Horio F, Ohno T, Namikawa T: Quantitative trait locus analysis of serum insulin, triglyceride, total cholesterol and phospholipids levels in the (SM/J × A/J)F_2 mice. *Exp Anim* 52:37–42, 2003
25. Ehrich TH, Kenney JP, Pletscher LS, Semenkovich CF, Cheverud JM: Fine-mapping gene by diet interactions in a LG/J×SM/J murine model of obesity. *Diabetes*. In press